PLOS ONE

RESEARCH ARTICLE

# Dual-source abdominopelvic computed tomography: Comparison of image quality and radiation dose of 80 kVp and 80/150 kVp with tin filter

**Seung Joon Choi[1☯], Su Joa Ahn[1☯], So Hyun Park[1]*, Seong Ho Park[2], Seong Yong Pak[3], Jae Won Choi[3], Young Sup Shim[1], Yu Mi Jeong[1], Bohyun Kim[4]**

**1** Department of Radiology, Gil Medical Center, Gachon University College of Medicine, Incheon, Korea, **2** Division of Abdominal Radiology, Department of Radiology and Research Institute of Radiology, Asan Medical Center, University of Ulsan College of Medicine, Seoul, Korea, **3** Imaging and Computer Vision Division, Siemens Healthcare, Seoul, Korea, **4** Department of Radiology, Seoul Saint Mary's Hospital, Seoul, Korea

☯ These authors contributed equally to this work.
* nnoleeter@naver.com





**Citation:** Choi SJ, Ahn SJ, Park SH, Park SH, Pak SY, Choi JW, et al. (2020) Dual-source abdominopelvic computed tomography: Comparison of image quality and radiation dose of 80 kVp and 80/150 kVp with tin filter. PLoS ONE 15 (9): e0231431. https://doi.org/10.1371/journal.pone.0231431

**Editor:** Dong-Hoon Lee, Yonsei University, South Korea, REPUBLIC OF KOREA

**Received:** April 4, 2020

**Accepted:** August 19, 2020

**Published:** September 3, 2020



**Data Availability Statement:** Data underlying the study cannot be made publicly available due to ethical concerns about sensitive patient information, as determined by the Gil Medical Center Research Ethics Committee. Data is available on request to the Ethics Committee (contact via Gil medical center's data access committee at irb@gilhospital.com) for researchers who meet the criteria for access to confidential data.

## Abstract

### Objective

To compare the radiation dose and the objective and subjective image quality of 80 kVp and 80/150 kVp with tin filter (80/Sn150 kVp) computed tomography (CT) in oncology patients.

### Methods

One-hundred-and-forty-five consecutive oncology patients who underwent third-generation dual-source dual-energy CT of the abdomen for evaluation of malignant visceral, peritoneal, extraperitoneal, and bone tumor were retrospectively recruited. Two radiologists independently reviewed each observation in 80 kVp CT and 80/Sn150 kVp CT. Modified line-density profile of the tumor and contrast-to-noise ratio (CNR) were measured. Diagnostic confidence, lesion conspicuity, and subjective image quality were calculated and compared between image sets. The effective dose and size-specific dose estimate (SSDE) were calculated in the image sets.

### Results

Modified line-density profile analysis revealed higher attenuation differences between the tumor and normal tissue in 80 kVp CT than in 80/Sn150 kVp CT (127 vs. 107, $P = 0.05$). The 80 kVp CT showed increased CNR in the liver (8.0 vs. 7.6) and the aorta (18.9 vs. 16.3) than the 80/Sn150 kVp CT. The 80 kVp CT yielded higher enhancement of organs (4.9 ± 0.2 vs. 4.7 ± 0.4, $P<0.001$) and lesion conspicuity (4.9 ± 0.3 vs. 4.8 ± 0.5, $P = 0.035$) than the 80/Sn150 kVp CT; overall image quality and confidence index were comparable. The effective dose was reduced by 45.2% with 80 kVp CT (2.3 mSv ± 0.9) compared to 80/Sn150 kVp CT

**Funding:** This research was supported by the Basic Science Research Program through the National Research Foundation of Korea and funded by the Ministry of Science ICT and Future Planning (2018R1C1B5044024) and the Gachon University research fund of 2017 (GCU-2017-5256).

**Competing interests:** NO authors have competing interests

**Abbreviations:** ADMIRE, advanced Modeled Iterative Reconstruction; ATVS, automated tube voltage selection; CNR, contrast-to-noise ratio; $CTDI_{vol}$, volumetric CT dose index; DLP, dose length product; DECT, dual-energy computed tomography; ED, Effective dose; HU, Hounsfield units; IR, iterative reconstruction; mGy, milligray; mSv, millisieverts; ROI, region of interest; SD, standard deviation; SNR, signal-to-noise ratio; SSDE, size-specific dose estimate.

(4.1 mSv ± 1.5). The SSDE was 7.4 ± 3.8 mGy on 80/Sn150 kVp CT and 4.1 ± 2.2 mGy on 80 kVp CT.

## Conclusions

The 80 kVp CT reduced the radiation dose by 45.2% in oncology patients while showing comparable or superior image quality to that of 80/Sn150 kVp CT for abdominal tumor evaluation.

## Introduction

Optimization of the radiation dose delivered in abdominopelvic computed tomography (CT) imaging is important, especially in situations where repeated CT examinations are performed in patients. Patients with malignancy undergo repeated CT examinations for evaluation of treatment response and surveillance after treatment. Various strategies have been developed to further reduce the radiation dose, including low kVp, automated exposure control, and iterative reconstruction (IR) [1,2]. Automatic tube current modulation (ATCM) can allow a reduction in the radiation exposure during CT examination, which is also affected by the patient's size [3,4]. Currently, 80 kVp is feasible and increasingly used as the optimal radiation dose [5–8]; however, although using a low kVp reduces the radiation dose, it increases the image noise [9]. IR selectively reduces statistical noise in the images, thereby improving the quality of subtle image details and may facilitate dose reduction. In the past decade, the evolution from statistical-based to model-based iterative algorithms has improved the performance of IR algorithms [10]. Advanced modelled iterative reconstruction (ADMIRE; Siemens Healthcare, Forchheim, Germany) is a model-based IR that can reduce noise in raw data and may allow further dose reduction while generating images of acceptable quality. ADMIRE is based on the results of the pseudo raw data, in comparison to the measured data, which is subtracted and reinserted into the loop afterward [11].

Dual-source dual-energy CT (DECT) systems enable dual-energy data to be acquired using two X-ray sources at different energy levels, i.e., a variety of voltage and tube current combinations [12–15]. Dual-source DECT images use a blend of low- and high-kVp images to provide an image impression similar to a standard 120 kV image (i.e., 80/140, 80/Sn150, or 90/Sn150 kVp) to generate virtual noncontrast images [14]. In other words, low kVp/high kVp with tin filter (Sn) CT generates low kVp, virtual noncontrast, and blended images, which are widely used in oncology [14]. In addition, virtual monochromatic images can be used to magnify the iodine contrast-to-noise ratio (CNR) to enhance the differentiation between tumor and background using DECT in oncology [15,16]. Although initial DECT revealed a three times higher radiation dose than single-energy CT [17], recent studies have demonstrated that third-generation dual-source DECTs can be performed without a radiation dose penalty or impairment of image quality compared to single-energy CT with 100–120 kVp [18,19]. They suggested that DECT can be routinely used in patients as there is no increase in the radiation dose compared to single-energy CT. However, no comparison has been reported between images with low kVp from single-energy CT and blending images from DECT. If the performance of an 80 kVp CT scan is similar to that of a blending image (80/Sn150 kVp) of DECT while reducing the radiation dose, it may reduce the use of DECT in patients who receive repetitive scans. To our knowledge, this imaging scheme concept has not been explored previously.

Thus, the purpose of our study was to compare the image quality and radiation dose between 80 kVp and 80/Sn150 kVp CT scans performed by the third-generation dual-source DECT using the ADMIRE reconstruction algorithm.

## Materials and methods

### Study design

This study was a retrospective analysis of CT images and was approved by our Institutional Review Board of Gil medical center with a waiver of the requirement for patient consent.

### Study patients

We screened 191 consecutive patients who were referred for CT examinations of the chest and abdominopelvic region between August 2018 and March 2019 for assessment of response to chemotherapy, or surveillance of treated malignancy. Abdominopelvic CT was selected for this study. The inclusion criteria were as follows: (a) solid nodules of malignant liver tumor, other malignant visceral tumors (except liver tumors), metastatic lymph nodes (larger than 1.5 cm along the short axis), peritoneal tumors, extraperitoneal tumors (i.e., retroperitoneum, muscle, subcutaneous fat layer), and metastatic bone tumors, (b) nodules $\leq$ 5 in number, and (c) nodules not typically hemangiomas or cysts. Six predetermined abdominopelvic lesions were modified from a previously described report [20]. We limited the number of nodules to minimize a cluster bias. We excluded 46 patients without a reference standard (MRI, PET/CT, or surgery), without any lesion on CT, or because of a change in protocol. Thus, 259 nodules in 145 consecutive patients were included (Fig 1). Nodules were selected and annotated by an experienced study coordinator (BLINDED-FOR-PEER-REVIEW), who was not involved in the image analysis.

### CT examination protocol

CT examinations were performed using a 192-slice, third-generation dual-source CT scanner (SOMATOM Force, Siemens Healthcare, Forchheim, Germany) in the dual-energy mode with tube detectors A (80 kVp; reference tube current, 250 mAs) and B (Sn 150 kVp; reference tube current, 125 mAs), using tube current dose modulation (CARE dose 4D; Siemens Healthcare) (Table 1).

### Data reconstruction

Images from 80/Sn150 kVp CT (data from tube detectors A and B) and 80 kVp CT (data from tube detector A) scans were made with an axial reconstruction thickness of 3 mm using the ADMIRE algorithm at a strength level of 2 out of 5, each with an edge-enhancing convolution kernel (Br64). The blended images were reconstructed by applying a blending factor of 0.6 (M_0.6; 60% of the 80 kVp and 40% of Sn 150 kVp spectrum). The reconstruction was achieved on a multimodality workstation (syngo.via VB20, Siemens Healthcare).

### CT data analysis

**Subjective analysis: Image quality and diagnostic confidence.** Two randomized image reading sessions were created based on the 80 kVp and 80/Sn150 kVp CT scans in which 290 examinations were anonymously reviewed by two independent board-certified radiologists (BLINDED-FOR-PEER-REVIEW, with 10 and 12 years of experience in abdominopelvic CT). A 6-week washout period was performed between reading sessions to minimize recall bias. After the sessions, a consensus between readers was used to settle discrepancies. The overall

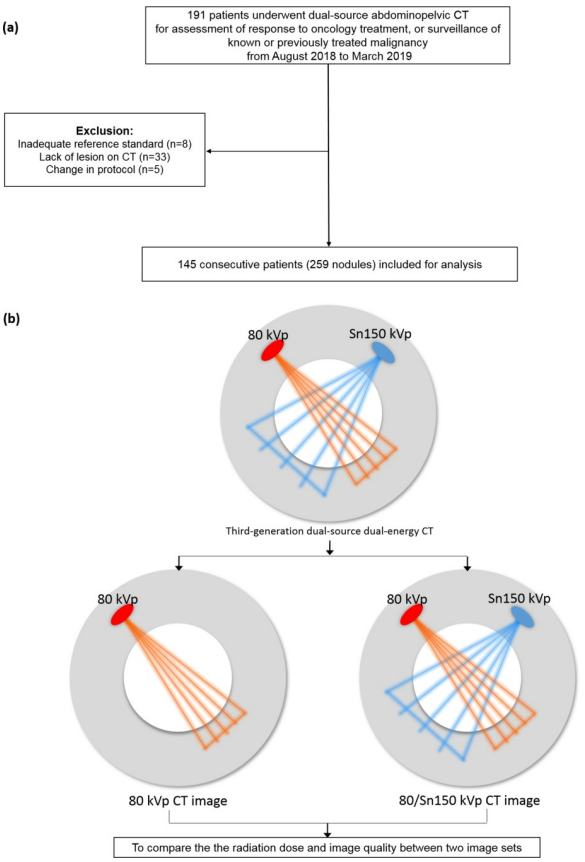


**Fig 1. Patient flow chart.** Selection process (a) and study design (b).

https://doi.org/10.1371/journal.pone.0231431.g001

image quality for diagnostic purposes was graded using a 5-point scale (1, nondiagnostic image quality, strong artefacts; 2, severe artefacts with uncertainty about the evaluation; 3, moderate artefacts with mild restricted assessment; 4, slight artefacts with unrestricted diagnostic image evaluation possible; and 5, excellent image quality with no artefacts).

**Table 1. CT acquisition scanning parameters.**

| | 80 kVp | 80/Sn150 kVp |
|---|---|---|
| Detector tube | A tube | Combination of A and B tube |
| Kilovolt | 80 | 80/Sn150 |
| Reference tube current (mAs) | 250 | 250/125 |
| Coverage | Lower lung fields ~ upper thigh | |
| Acquisition mode | Helical | Helical |
| Automated tube current modulation | On | On |
| Automated tube voltage selection | Off | Off |
| Pitch | 1.15 | 1.15 |
| Rotation time (sec) | 0.5 | 0.5 |
| Reconstruction algorithm | ADMIRE | ADMIRE |
| Reconstructed slice thickness | 3 mm | 3 mm |

ADMIRE, advanced modelled iterative reconstruction.

https://doi.org/10.1371/journal.pone.0231431.t001

Enhancement of organs was graded using a 5-point scale (1, very poor; 2, suboptimal; 3, acceptable; 4, above average; and 5, excellent). Image noise was graded using a 5-point scale (1, unacceptably high; 2, higher than average; 3, average; 4, less than average; and 5, minimum noise). A score was derived for axial images with a soft-tissue window setting (width, 400 HU; level, 50 HU) on a PACS system. Reviewers were allowed to change the window level and width as per their comfort level during analysis.

For each presented acquisition, both readers had to independently assess the predetermined abdominopelvic lesions. Each item was graded using a five-point confidence index (1, very poor; 2, poor; 3, average; 4, high; and 5, excellent confidence) and an ordinal scale for lesion conspicuity (1, definite artefact [pseudolesion]; 2, probable artefact; 3, subtle lesion; 4, poorly visualized margins; and 5, well-visualized margins). A score of either 1 or 2 was considered unacceptable for diagnostic purposes.

**Objective image analysis.** Image noise was measured by drawing a circular region of interest (ROI; size between 1 and 3 $cm^2$), as standard deviations (SDs) in Hounsfield units (HU), on the axial images of two image sets in the following three anatomical regions by one blinded reader (BLINDED-FOR-PEER-REVIEW) [21–23]: the subcutaneous fat in the anterior abdominal wall, the right hepatic lobe parenchyma, and the lumen of abdominal aorta. Mean attenuation values were measured (in HU) for each ROI in all image sets. Signal-to-noise ratio (SNR = mean HU of interested area/fat noise) and CNR ([mean HU of interested area—mean HU of psoas muscle]/ fat noise) were calculated [9,20]. Fat noise was calculated as the mean of standard deviation of CT attenuation in ROIs placed within the mesenteric fat. ROIs were carefully placed at the same location between different image series.

The two image sets were used for modified line-density analysis [24]. The tumor was identified on 80/Sn150 images, and one reader, with 4 years of experience, positioned a line of 10 mm in length and 2 mm in width perpendicular to the tumor margins with one half of the line within the tumor and the other half within the normal tissue. Mean, minimum, and maximum HU values were measured within this 10-mm line using a multimodality workstation. Modified line-density analysis was performed on 128 nodules from 92 patients, as not available in patients with peritoneal seeding lesions.

## Radiation dose

The dose-length product (DLP) and volume CT Dose Index ($CTDI_{vol}$) were recorded from the scanner dose page. The effective dose (in millisieverts, mSv) was calculated using the tissue-weighting factor (men, $k = 0.012$; women, $k = 0.017$) based on the International Commission on Radiological Protection Publication 103 with modifications [25,26] as follows:

$$\text{effective dose} = \text{DLP} \times \text{tissue} - \text{weighting factor}$$

Size-specific dose estimates (SSDEs) were calculated as follows:

$$\text{SSDE} = \text{CTDI}_{\text{vol}} \times \text{conversion factor}$$

A conversion factor based on the effective diameter and a 32-cm-diameter polymethylmethacrylate phantom was used [27]. The effective diameter was calculated from the anteroposterior (AP) and lateral dimensions on the CT scan as follows:

$$\text{effective diameter} = \sqrt{AP \times \text{lateral dimention}} \quad [27]$$

### Statistical analysis

Dose parameters and image analysis were compared between different dose CT scans using Student's t-test and chi-squared test. The interobserver agreement between the two readers for each of the evaluated subjective image quality parameter was estimated using the overall proportion of agreement [28], rather than κ statistics, as the latter is affected by the distribution of data across categories and was thus not a valid indicator of our data [29]. A *P*-value <0.05 was considered statistically significant. All statistical analyses were performed using SPSS Statistics for Windows, Version 21.0 (IBM Corp.).

## Results

### Patient characteristics

Of the 145 patients in our study, 79 (54.5%) were men and 66 (45.5%) were women with a mean age ± standard deviation of 62.4 ± 10.5 years. The body mass index (BMI) ranged from 15.1 to 30.7 kg/m$^2$ (mean, 22.8 kg/m$^2$; median, 22.5 kg/m$^2$). Altogether, 259 nodules were included in the analysis: 98 malignant nodules in the liver, 55 peritoneal seeding nodules, 45 metastatic bone tumors, 31 metastatic lymph nodes, 23 other visceral tumors, and 7 extraperitoneal tumors (Table 2).

### Objective image quality

The 80 kVp CT had a significantly higher attenuation compared to 80/Sn150 kVp CT in the liver and aorta (125.9 HU vs. 107.2 HU, *P*<0.001; 208.2 HU vs. 160.5 HU, *P*<0.001; Table 3 and Fig 2). The CNR of the aorta in 80 kVp CT images was significantly higher than in 80/Sn150 kVp CT images (*P*<0.001) whereas the CNR of the liver in 80 kVp CT images was mildly higher than that in 80/Sn150 kVp CT images (*P* = 0.197). The SNR of the liver and aorta tended to be higher in 80/Sn150 kVp CT images, although there was no significant difference between the image sets (*P* = 0.075 and 0.069, respectively).

The mean differences between maximum and minimum attenuation within the tumor are shown in Table 4. The mean attenuation differences within the tumor in 80 kVp CT were significantly higher than those in 80/Sn150 kVp CT (127.2 HU vs. 107.0 HU, *P* = 0.05).

### Subjective image quality

The 80 kVp CT showed a significantly higher enhancement of organs (4.9 ± 0.2 vs. 4.7 ± 0.4, *P*<0.001) and lesion conspicuity (4.9 ± 0.3 vs. 4.8 ± 0.5, *P* = 0.035) than 80/Sn150 kVp CT according to the consensus interpretation, as well as similar overall image quality (4.8 ± 0.3 vs. 4.9 ± 0.2) and confidence index (4.8 ± 0.5 vs. 4.8 ± 0.6; Figs 3 and 4 and Table 5).

### Reader agreement

Interobserver agreement between the two readers for overall image quality, enhancement of organs, image noise, confidence index, and lesion conspicuity were 85.5%, 92.0%, 87.2%, 89.1%, and 84.3%, respectively.

### Radiation dose

Various dose parameters of the two image sets are shown in Table 6 and Fig 5. For the 80/Sn150 kVp CT, the mean $CTDI_{vol}$ was 5.3 ± 1.4 mGy, and the SSDE was 7.4 ± 3.8 mGy, with an effective dose of 4.1 ± 1.5 mSv. For the 80 kVp CT, the mean $CTDI_{vol}$ was 2.9 ± 1.0 mGy, and the SSDE was 4.1 ± 2.2 mGy, with an effective dose of 2.3 ± 0.9 mSv. On average, the

**Table 2. Patient information.**

| Parameter | Value |
|---|---|
| **Patients, (n = 145)** | |
| Age (years) * | |
| All patients (men: women = 79: 66) | 62.4 ± 10.5 |
| Height (cm) * | 163.1 ± 8.2 |
| Weight (kg) * | 60.2 ± 12.6 |
| Effective diameter (cm) * | 26.2 ± 2.9 |
| Body mass index (BMI) * | 22.8 ± 4.0 |
| <18.5 (underweight) | 23 (15.9) |
| 18.5–24.9 (normal) | 81 (55.9) |
| 25–29.9 (overweight) | 33 (22.8) |
| 30–34.9 (moderately obese) | 6 (4.1) |
| 35–39.9 (severely obese) | 2 (1.4) |
| Type of primary cancer | |
| Colorectal | 47 (32.4) |
| Hepatobiliary | 25 (17.2) |
| Gastro-small bowel | 24 (16.5) |
| Breast | 17 (11.7) |
| Genitourinary | 14 (9.7) |
| Bronchial | 8 (5.5) |
| Others | 10 (6.9) |
| Reference standard | |
| Liver MRI and PET/CT | 48 (33.1) |
| PET/CT | 37 (25.5) |
| Pelvis MRI and PET/CT | 18 (12.4) |
| PET/CT and spine MRI | 17 (11.7) |
| Liver MRI, PET/CT, and surgery | 15 (10.3) |
| Liver MRI, PET/CT, and spine MRI | 7 (4.8) |
| Liver MRI and surgery | 3 (2.0) |

Data are presented as number (%), unless indicated otherwise.

* Data are means ± standard deviations.

MRI, magnetic resonance imaging; PET, positron emission tomography; CT, computed tomography

https://doi.org/10.1371/journal.pone.0231431.t002

effective dose of 80 kVp CT scan was 45.2% ± 2.8% (range, 38.0–51.9%) less than that of 80/Sn150 kVp CT.

## Discussion

We investigated whether the performance of 80 kVp CT was comparable to that of the 80/Sn150 kVp CT while reducing the radiation dose, to ascertain if it could be used in oncology patients who receive repetitive DECT scans. Our findings revealed that there was a 45.2% reduction in radiation dose by using the low tube voltage (80 kVp) CT imaging with ADMIRE while maintaining excellent image quality compared with DECT (80/Sn150 kVp). Contrast-related features including enhancement of organs, CNR, and attenuation differences within the tumor border were higher in 80 kVp CT than in 80/Sn150 kVp CT, while SNR showed no significant differences. A potential explanation for these findings is that lowering the CT tube voltage results in a greater photoelectric effect of iodinated contrast media, with only a slight

**Table 3. Assessment of objective image quality.**

| Quantitative analysis (Hounsfield units) | 80 kVp CT | 80/Sn150 kVp CT | *P*-value |
|---|---|---|---|
| Attenuation | | | |
| Right hepatic lobe | 125.9 ± 19.4 | 107.2 ± 15.2 | < 0.001 |
| Abdominal aorta | 208.2 ± 30.5 | 160.5 ± 22.5 | < 0.001 |
| Noise | | | |
| Right hepatic lobe | 10.5 ± 2.1 | 8.0 ± 1.4 | < 0.001 |
| Abdominal aorta | 12.1 ± 2.1 | 9.3 ± 1.5 | < 0.001 |
| Contrast-to-noise ratio | | | |
| Right hepatic lobe | 8.0 ± 3.1 | 7.6 ± 3.0 | 0.197 |
| Abdominal aorta | 18.9 ± 5.5 | 16.3 ± 5.0 | < 0.001 |
| Signal-to-noise ratio | | | |
| Right hepatic lobe | 16.6 ± 4.0 | 17.5 ± 3.9 | 0.075 |
| Abdominal aorta | 27.5 ±6.5 | 26.2 ± 6.1 | 0.069 |

CT, computed tomography.

Data shown are mean ± standard deviation

https://doi.org/10.1371/journal.pone.0231431.t003

increase in the noise because of improved tube current capabilities. Moreover, the advances in hardware equipped with Stellar detectors and software program in third-generation dual-source CT [30,31], which are supposed to be more sensitive to electron influx, are thus, dose-efficient and generate high quality images while using 80 kVp. A few studies that investigated DECT, showed that the radiation dose was comparable to the single energy 100–120 kVp CT [18,32]. However, our study found that the 80 kVp CT showed superior image quality with a lower radiation dose than DECT in abdominal scans. Thus, DECT should not be routinely used in patients who may require repeated abdominopelvic CT scans.

Several studies have reported that 80 kVp abdominopelvic CT can be used effectively while reducing radiation dose in patients with a normal BMI [33–36]. Studies have also reported that reducing the tube voltage from 120 kVp to 80 kVp resulted in a 48–65% dose reduction using either an identical tube current or automated tube current modulation [37–39]. However, extremely low tube voltage scans may result in noisier images that are inadequate for interpretation. An increase in tube current or use of IR may improve image quality and lesion

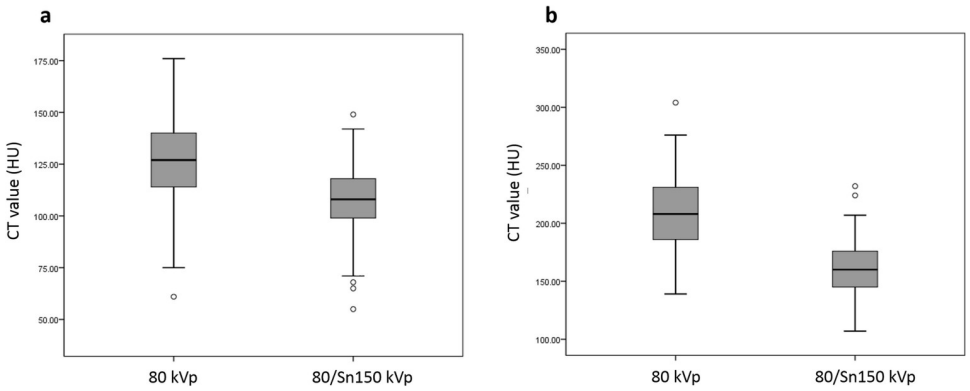


**Fig 2. Box and whisker plots of CT enhancement.** Difference in the liver parenchyma (a) and abdominal aorta (b) between 80 kVp and 80/Sn150 kVp CT. Box-and-whisker diagrams show mean values ± standard deviation, as well as minimum and maximum values.

https://doi.org/10.1371/journal.pone.0231431.g002

**Table 4. Differences between modified line-density profiles within the tumor border.**

| Hounsfield units | 80 kVp | 80/Sn150 kVp | *P*-value |
|---|---|---|---|
| Mean ± SD | 127.2 ± 71.9 | 107.0 ± 59.4 | 0.05 |
| Maximum | 882 | 726 | |
| Minimum | -66 | -54 | |

The difference was defined as the maximum Hounsfield units – minimum Hounsfield units. SD, standard deviation

https://doi.org/10.1371/journal.pone.0231431.t004

conspicuity [30]. Our study showed that the effective dose of 80 kVp CT (2.3 mSv ± 0.9) scan was 45.2% less than that of 80/Sn150 kVp CT (4.1 mSv ± 1.5) using IR. Low tube-voltage CT scan is a robust method for radiation dose reduction in abdominopelvic CT.

Third-generation dual-source CT is more dose-efficient than second-generation dual-source CT because of technical advances and adjusted scan protocols while the image quality is consistently high with all assessed protocols [36]. The low kVp is more likely selected while using automated tube voltage selection (ATVS), thereby reducing the radiation dose in third-generation dual-source CT. Park et al. reported that third generation dual-source CT demonstrated an increase in the number of 90–100 kVp CTs, whereas the majority of the patients underwent 100–120 kVp using ATVM on second generation dual-source CT [36]. Winklehner et al. reported that using third-generation dual-source CT, compared to second-generation, resulted in a tube voltage decrease of at least 10 kV in most patients (75%, 100–90 kVp) who received body CT angiography examinations [39]. These results support the use of low kVp

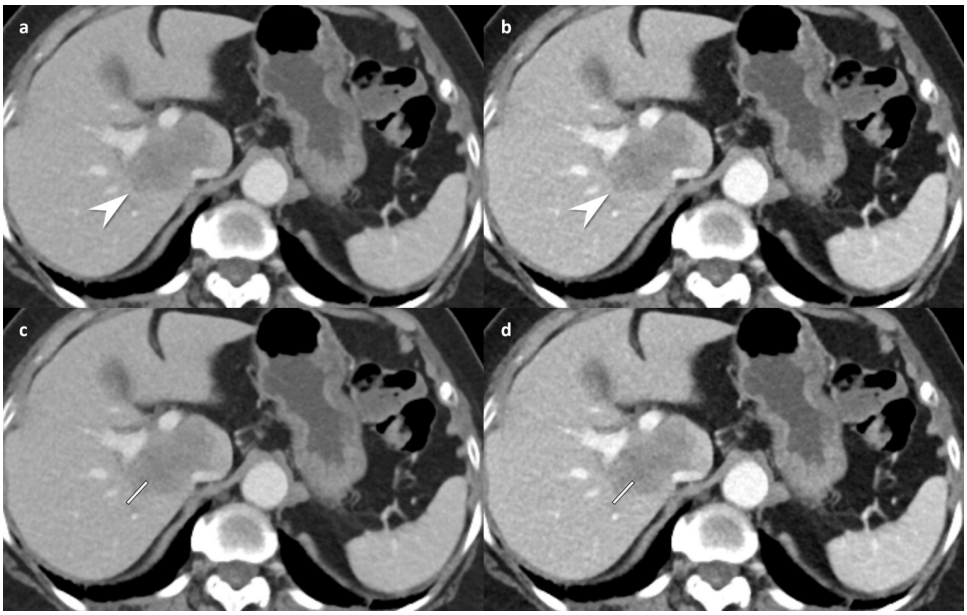


**Fig 3. Contrast-enhanced abdomen CT in portal venous phase in a 37-year-old woman (body mass index, 29.0 kg/m$^2$) with ascending colon cancer and liver metastasis.** 80/Sn150 kVp CT (a, effective dose; 5.9 mSv) shows a liver metastasis in the right hepatic lobe/segment 1 (white arrowhead) by each reader (reader 1 and reader 2, grade 4 lesion conspicuity, grade 5 diagnostic confidence, and grade 5 overall image quality). The corresponding image obtained during the same contrast-enhanced phase with 80 kVp CT (b, effective dose; 3.4 mSv) demonstrates increased conspicuity of the lesion by each reader (white arrowhead, reader 1 and reader 2, grade 5 lesion conspicuity, grade 5 diagnostic confidence, and grade 5 overall image quality). Modified line-density profile revealed higher attenuation differences between the tumor and the normal tissue at 80 kVp (d) than those at 80/Sn150 CT (c) (maximum HU: minimum HU, 157:52 vs.129:49). CT, computed tomography.

https://doi.org/10.1371/journal.pone.0231431.g003

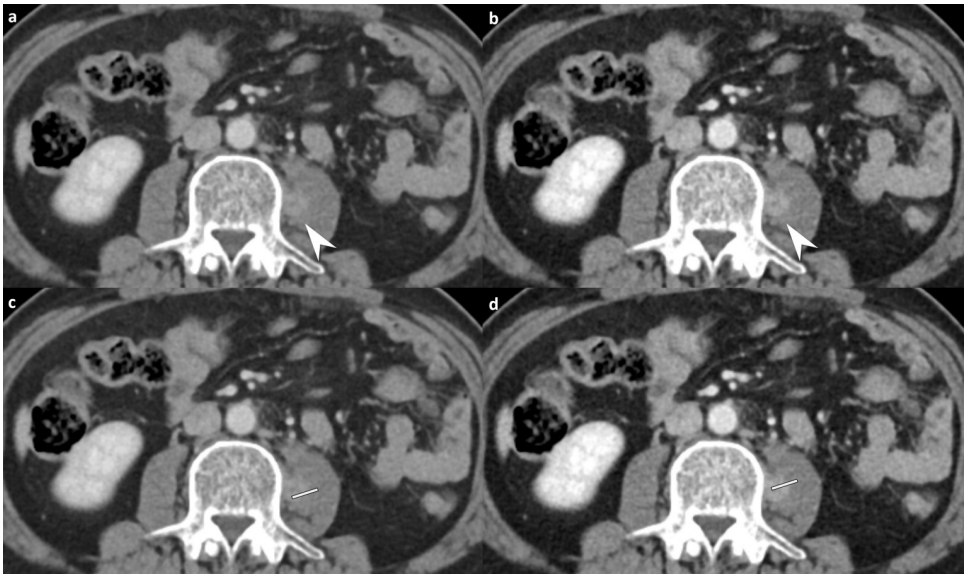


**Fig 4. Contrast-enhanced abdomen CT in the portal venous phase in a 45-year-old man (body mass index, 24.8 kg/m$^2$) with sigmoid colon cancer with a seeding nodule in the left psoas muscle.** 80/Sn150 kVp CT (a-b, effective dose; 4.5 mSv) showing a hyperattenuating mass in the left psoas muscle (white arrows) by each reader (reader 1 and reader 2, grade 4 lesion conspicuity, grade 5 diagnostic confidence, and grade 5 overall image quality). The corresponding image obtained during the identical phase with 80 kVp CT (effective dose; 2.6 mSv) demonstrates markedly increased conspicuity of the lesion in the left psoas muscle by each reader (reader 1 and reader 2, grade 5 lesion conspicuity, grade 5 diagnostic confidence, and grade 5 overall image quality). Modified line-density profile revealed higher attenuation differences between the tumor and the normal tissue at 80 kVp (d) than those at 80/Sn150 CT (c) (maximum HU: minimum HU, 129:27 vs.106:36). CT, computed tomography.

https://doi.org/10.1371/journal.pone.0231431.g004

abdominopelvic CT in patients for reducing the radiation dose as well as for maintaining the diagnostic performance employed in our study.

The low tube-voltage CT technique improves tumor conspicuity and tumor-to-tissue CNR [5,6]. In our study, mean differences between the maximum and minimum attenuation within the tumor was 127.2 HU in 80 kVp CT and 107.0 HU in 80/Sn150 kVp CT. Our results also demonstrated that the 80 kVp CT scan might be preferred over 80/Sn150 kVp CT for detecting hypervascular tumors because of better scores in all contrast-related features, increased enhancement of organs, CNR, and attenuation differences within the tumor border. The lesion conspicuity was slightly higher in 80 kVp CT compared to 80/Sn150 kVp CT, which means that low-density lesion detection is superior in 80 kVp CT compared to that in 80/Sn150 kVp CT. However, SNR of the liver and the aorta showed no significant difference between the

**Table 5. Assessment of subjective image quality.**

| | 80 kVp CT | 80/Sn150 kVp CT | *P*-value |
|---|---|---|---|
| Overall image quality | 4.8 ± 0.3 | 4.9 ± 0.2 | 0.306 |
| Enhancement of organs | 4.9 ± 0.2 | 4.7 ± 0.4 | < 0.001 |
| Image noise | 4.8 ± 0.3 | 4.9 ± 0.1 | 0.061 |
| Confidence index | 4.8 ± 0.5 | 4.8 ± 0.6 | 0.687 |
| Lesion conspicuity | 4.9 ± 0.3 | 4.8 ± 0.5 | 0.035 |

CT, computed tomography.

Data shown are mean ± standard deviation

https://doi.org/10.1371/journal.pone.0231431.t005

**Table 6. Dose parameters of each image set.**

| | 80 kVp | 80/Sn150 kVp | *P*-value |
|---|---|---|---|
| $CTDI_{vol}$ (mGy) | 2.9 ± 1.0 (1.3–8.1) | 5.3 ±1.4 (2.8–12.7) | < 0.001 |
| DLP (mGy-cm) | 159.6 ± 61.9 (61.7–493.3) | 287.1 ± 94.8 (128.0–752.0) | < 0.001 |
| Effective dose (mSv) | 2.3 ± 0.9 (0.7–5.9) | 4.1 ± 1.5 (1.5–9.5) | < 0.001 |
| SSDE (mGy) | 4.1 ± 2.2 (2.4–8.1) | 7.4 ± 3.8 (5.0–12.3) | < 0.001 |

Data are means ± standard deviations.

$CTDI_{vol}$, volume CT dose index; mGy, milligray; DLP, dose-length product; mSv, millisieverts; SSDE, size-specific dose estimate.

https://doi.org/10.1371/journal.pone.0231431.t006

image sets in our study. Our results showed a balance between image noise and low-density lesion detectability while using low tube-voltage CT to evaluate solid organs.

DECT of the abdomen has the advantage of analyzing CT images in various ways, including monoenergetic image analysis, liver fat and iron quantification, urinary calculi characterization, and gallstone imaging [15,37,38]. Another advantage of DECT is the faster acquisition time to discern the hemodynamic features from a moving organ (i.e., cardiac study) [40,41]. Unlike previous studies [18,32] that suggested the routine use of DECT, our study found that the performance alone was not sufficient to justify routine use of DECT for oncology patients who frequently undergo CT examinations, sometimes every 1–2 months, because the radiation dose is higher with 80/Sn150 kVp CT compared to 80 kVp CT. Moreover, we reported superior tissue contrast features with 80 kVp CT.

Our study had some limitations. First, it was a retrospective study involving oncology patients with a tumor lesion on abdominopelvic CT, which may have introduced a selection bias. Second, our study had a small number of patients with moderate to severe obesity; thus, we could not perform a robust comparison between 80/Sn150 kVp and 80 kVp CT in patients with moderate to severe obesity. Third, 80/Sn150 kVp scan combines 80 kVp and Sn 150 kVp to generate the image; therefore, 80/Sn150 kVp was set to have an unconditional higher radiation dose than 80 kVp scan. However, our aim was to focus on evaluating image quality between a low kVp image using single-energy scan and a blended image generated using DECT scan. Rather than increasing the radiation exposure of the patient through two scans, we considered that an intraindividual comparison would be ethical. Finally, we only evaluated the performance of a single low kVp image and a blended image in a single scan. We did not

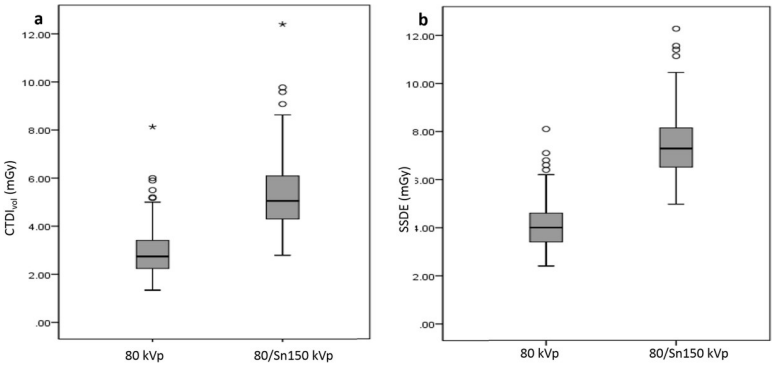


**Fig 5.** Box and whisker plots of $CTDI_{vol}$ (a) and SSDE (b) for 80 kVp and 80/Sn150 kVp scans. Box-and-whisker diagrams show mean values ± standard deviation, as well as minimum and maximum values.

https://doi.org/10.1371/journal.pone.0231431.g005

compare the image quality between a single energy CT and another data set from dual energy CT. Various combinations of sequences can build distinctive protocols of 80/140 kVp, 90/Sn150 kVp, and 90/Sn150 kVp compared with a 70–100 kVp CT scan.

## Conclusions

In conclusion, 80 kVp CT showed a decrease in radiation dose exposure while providing comparable or superior image quality to that of 80/Sn150 kVp CT in oncology patients.

## Supporting information

**S1 Appendix. STROBE checklist.**
(DOC)

**S1 Fig.**
(TIF)

**S2 Fig.**
(TIF)

## Author Contributions

**Conceptualization:** Seong Ho Park.

**Data curation:** Jae Won Choi.

**Formal analysis:** Seung Joon Choi, Su Joa Ahn.

**Funding acquisition:** So Hyun Park.

**Methodology:** Seong Ho Park, Young Sup Shim, Yu Mi Jeong.

**Software:** Seong Yong Pak.

**Visualization:** Seong Yong Pak.

**Writing – original draft:** So Hyun Park.

**Writing – review & editing:** Young Sup Shim, Yu Mi Jeong, Bohyun Kim.

## References

1. McCollough CH, Primak AN, Braun N, Kofler J, Yu L, Christner J. Strategies for reducing radiation dose in CT. Radiol Clin North Am. 2009; 47: 27–40. https://doi.org/10.1016/j.rcl.2008.10.006 PMID: 19195532
2. Marin D, Nelson RC, Schindera ST, Richard S, Youngblood RS, Yoshizumi TT, et al. Low-tube-voltage, high-tube-current multidetector abdominal CT: improved image quality and decreased radiation dose with adaptive statistical iterative reconstruction algorithm—initial clinical experience. Radiology. 2010; 254: 145–153. https://doi.org/10.1148/radiol.09090094 PMID: 20032149
3. Ang W, Hashim S, Karim M, Bahruddin N, Salehhon N, Musa Y, editors. Adaptive iterative dose reduction (AIDR) 3D in low dose CT abdomen-pelvis: Effects on image quality and radiation exposure. Journal of Physics: Conference Series; 2017: IOP Publishing.
4. Sabarudin A, Siong TW, Chin AW, Hoong NK, Karim MKA. A comparison study of radiation effective dose in ECG-Gated Coronary CT Angiography and calcium scoring examinations performed with a dual-source CT scanner. 2019; 9: 4374. https://doi.org/10.1038/s41598-019-40758-5 PMID: 30867480
5. Marin D, Nelson RC, Samei E, Paulson EK, Ho LM, Boll DT, et al. Hypervascular liver tumors: low tube voltage, high tube current multidetector CT during late hepatic arterial phase for detection—initial clinical experience. Radiology. 2009; 251: 771–779. https://doi.org/10.1148/radiol.2513081330 PMID: 19346514

6. Marin D, Nelson RC, Barnhart H, Schindera ST, Ho LM, Jaffe TA, et al. Detection of pancreatic tumors, image quality, and radiation dose during the pancreatic parenchymal phase: effect of a low-tube-voltage, high-tube-current CT technique—preliminary results. Radiology. 2010; 256: 450–459. https://doi.org/10.1148/radiol.10091819 PMID: 20656835

7. Kaza RK, Platt JF, Al-Hawary MM, Wasnik A, Liu PS, Pandya A. CT enterography at 80 kVp with adaptive statistical iterative reconstruction versus at 120 kVp with standard reconstruction: image quality, diagnostic adequacy, and dose reduction. AJR Am J Roentgenol. 2012; 198: 1084–1092. https://doi.org/10.2214/AJR.11.6597 PMID: 22528897

8. Nakaura T, Nakamura S, Maruyama N, Funama Y, Awai K, Harada K, et al. Low contrast agent and radiation dose protocol for hepatic dynamic CT of thin adults at 256-detector row CT: effect of low tube voltage and hybrid iterative reconstruction algorithm on image quality. Radiology. 2012; 264: 445–454. https://doi.org/10.1148/radiol.12111082 PMID: 22627597

9. Ha HI, Hong SS, Kim M-J, Lee K. 100 kVp low-tube voltage abdominal CT in adults: radiation dose reduction and image quality comparison of 120 kVp abdominal CT. Journal of the Korean Society of Radiology. 2016; 75: 285–295. https://doi.org/10.3348/jksr.2016.75.4.285

10. Liu L. Model-based Iterative Reconstruction: A Promising Algorithm for Today's Computed Tomography Imaging. J Med Imaging Radiat Sci. 2014; 45: 131–136. https://doi.org/10.1016/j.jmir.2014.02.002 PMID: 31051943

11. Schaller F, Sedlmair M, Raupach R, Uder M, Lell M. Noise Reduction in Abdominal Computed Tomography Applying Iterative Reconstruction (ADMIRE). Acad Radiol. 2016; 23: 1230–1238. https://doi.org/10.1016/j.acra.2016.05.016 PMID: 27318787

12. Shim YS, Park SH. Comparison of submillisievert CT with standard-dose CT for urolithiasis. 2019: 284185119890088. https://doi.org/10.1177/0284185119890088 PMID: 31795730

13. Lee KH, Shim YS, Park SH. Comparison of standard-dose and half-dose dual-source abdominopelvic CT scans for evaluation of acute abdominal pain. 2019; 60: 946–954. https://doi.org/10.1177/0284185118809544 PMID: 30376718

14. Krauss B, Grant KL, Schmidt BT, Flohr TG. The importance of spectral separation: an assessment of dual-energy spectral separation for quantitative ability and dose efficiency. Invest Radiol. 2015; 50: 114–118. https://doi.org/10.1097/RLI.0000000000000109 PMID: 25373305

15. Marin D, Boll DT, Mileto A, Nelson RC. State of the art: dual-energy CT of the abdomen. Radiology. 2014; 271: 327–342. https://doi.org/10.1148/radiol.14131480 PMID: 24761954

16. Beer L, Toepker M, Ba-Ssalamah A, Schestak C, Dutschke A, Schindl M, et al. Objective and subjective comparison of virtual monoenergetic vs. polychromatic images in patients with pancreatic ductal adenocarcinoma. Eur Radiol. 2019; 29: 3617–3625. https://doi.org/10.1007/s00330-019-06116-9 PMID: 30888484

17. Ho LM, Yoshizumi TT, Hurwitz LM, Nelson RC, Marin D, Toncheva G, et al. Dual energy versus single energy MDCT: measurement of radiation dose using adult abdominal imaging protocols. Acad Radiol. 2009; 16: 1400–1407. https://doi.org/10.1016/j.acra.2009.05.002 PMID: 19596594

18. Wichmann JL, Hardie AD, Schoepf UJ, Felmly LM, Perry JD, Varga-Szemes A, et al. Single- and dual-energy CT of the abdomen: comparison of radiation dose and image quality of 2nd and 3rd generation dual-source CT. Eur Radiol. 2017; 27: 642–650. https://doi.org/10.1007/s00330-016-4383-6 PMID: 27165140

19. Uhrig M, Simons D, Kachelriess M, Pisana F, Kuchenbecker S, Schlemmer HP. Advanced abdominal imaging with dual energy CT is feasible without increasing radiation dose. Cancer Imaging. 2016; 16: 15. https://doi.org/10.1186/s40644-016-0073-5 PMID: 27329159

20. Leyendecker P, Faucher V, Labani A, Noblet V, Lefebvre F, Magotteaux P, et al. Prospective evaluation of ultra-low-dose contrast-enhanced 100-kV abdominal computed tomography with tin filter: effect on radiation dose reduction and image quality with a third-generation dual-source CT system. Eur Radiol. 2019; 29: 2107–2116. https://doi.org/10.1007/s00330-018-5750-2 PMID: 30324392

21. Morimoto LN, Kamaya A, Boulay-Coletta I, Fleischmann D, Molvin L, Tian L, et al. Reduced dose CT with model-based iterative reconstruction compared to standard dose CT of the chest, abdomen, and pelvis in oncology patients: intra-individual comparison study on image quality and lesion conspicuity. Abdom Radiol (NY). 2017; 42: 2279–2288. https://doi.org/10.1007/s00261-017-1140-5 PMID: 28417170

22. Pickhardt PJ, Lubner MG, Kim DH, Tang J, Ruma JA, del Rio AM, et al. Abdominal CT with model-based iterative reconstruction (MBIR): initial results of a prospective trial comparing ultralow-dose with standard-dose imaging. AJR Am J Roentgenol. 2012; 199: 1266–1274. https://doi.org/10.2214/AJR.12.9382 PMID: 23169718

23. Karpitschka M, Augart D, Becker HC, Reiser M, Graser A. Dose reduction in oncological staging multidetector CT: effect of iterative reconstruction. Br J Radiol. 2013; 86: 20120224. https://doi.org/10.1259/bjr.20120224 PMID: 23255541

24. Beer L, Toepker M, Ba-Ssalamah A, Schestak C, Dutschke A, Schindl M, et al. Objective and subjective comparison of virtual monoenergetic vs. polychromatic images in patients with pancreatic ductal adenocarcinoma. European radiology. 2019: 1–9.

25. J. V. The 2007 recommendations of the International Commission on Radiological Protection: Elsevier Oxford; 2007.

26. Goo HW. CT radiation dose optimization and estimation: an update for radiologists. Korean J Radiol. 2012; 13: 1–11. https://doi.org/10.3348/kjr.2012.13.1.1 PMID: 22247630

27. #204. CTSTG. Size specific dose estimates in pediatric and adult body CT examinations. [cited Jan 13th 2019]. Available: https://www.aapm.org/pubs/reports/rpt_204.pdf.

28. Kundel HL, Polansky M. Measurement of observer agreement. Radiology. 2003; 228: 303–308. https://doi.org/10.1148/radiol.2282011860 PMID: 12819342

29. Feinstein AR, Cicchetti DV. High agreement but low kappa: I. The problems of two paradoxes. J Clin Epidemiol. 1990; 43: 543–549. https://doi.org/10.1016/0895-4356(90)90158-l PMID: 2348207

30. Seyal AR, Arslanoglu A, Abboud SF, Sahin A, Horowitz JM, Yaghmai V. CT of the Abdomen with Reduced Tube Voltage in Adults: A Practical Approach. Radiographics. 2015; 35: 1922–1939. https://doi.org/10.1148/rg.2015150048 PMID: 26473536

31. Tabari A, Lo Gullo R, Murugan V, Otrakji A, Digumarthy S, Kalra M. Recent Advances in Computed Tomographic Technology: Cardiopulmonary Imaging Applications. J Thorac Imaging. 2017; 32: 89–100. https://doi.org/10.1097/RTI.0000000000000258 PMID: 28221262

32. Schmidt D, Soderberg M, Nilsson M, Lindvall H, Christoffersen C, Leander P. Evaluation of image quality and radiation dose of abdominal dual-energy CT. Acta Radiol. 2018; 59: 845–852. https://doi.org/10.1177/0284185117732806 PMID: 28927299

33. Raman SP, Johnson PT, Deshmukh S, Mahesh M, Grant KL, Fishman EK. CT dose reduction applications: available tools on the latest generation of CT scanners. J Am Coll Radiol. 2013; 10: 37–41. https://doi.org/10.1016/j.jacr.2012.06.025 PMID: 23290672

34. Del Gaizo AJ, Fletcher JG, Yu L, Paden RG, Spencer GC, Leng S, et al. Reducing radiation dose in CT enterography. Radiographics. 2013; 33: 1109–1124. https://doi.org/10.1148/rg.334125074 PMID: 23842974

35. Sigal-Cinqualbre AB, Hennequin R, Abada HT, Chen X, Paul JF. Low-kilovoltage multi-detector row chest CT in adults: feasibility and effect on image quality and iodine dose. Radiology. 2004; 231: 169–174. https://doi.org/10.1148/radiol.2311030191 PMID: 15068946

36. Park C, Gruber-Rouh T, Leithner D, Zierden A, Albrecht MH, Wichmann JL, et al. Single-source chest-abdomen-pelvis cancer staging on a third generation dual-source CT system: comparison of automated tube potential selection to second generation dual-source CT. 2016; 16: 33. https://doi.org/10.1186/s40644-016-0093-1 PMID: 27724954

37. Karcaaltincaba M, Aktas A. Dual-energy CT revisited with multidetector CT: review of principles and clinical applications. Diagn Interv Radiol. 2011; 17: 181–194. https://doi.org/10.4261/1305-3825.DIR.3860-10.0 PMID: 20945292

38. Parakh A, Macri F, Sahani D. Dual-Energy Computed Tomography: Dose Reduction, Series Reduction, and Contrast Load Reduction in Dual-Energy Computed Tomography. Radiol Clin North Am. 2018; 56: 601–624. https://doi.org/10.1016/j.rcl.2018.03.002 PMID: 29936950

39. Winklehner A, Gordic S, Lauk E, Frauenfelder T, Leschka S, Alkadhi H, et al. Automated attenuation-based tube voltage selection for body CTA: Performance evaluation of 192-slice dual-source CT. Eur Radiol. 2015; 25: 2346–2353. https://doi.org/10.1007/s00330-015-3632-4 PMID: 25693663

40. Danad I, Ó Hartaigh B, Mi JK. Dual-energy computed tomography for detection of coronary artery disease. Expert review of cardiovascular therapy. 2015; 13: 1345–1356. https://doi.org/10.1586/14779072.2015.1102055 PMID: 26549789

41. Danad I, Fayad ZA, Willemink MJ, Min JK. New Applications of Cardiac Computed Tomography: Dual-Energy, Spectral, and Molecular CT Imaging. JACC Cardiovascular imaging. 2015; 8: 710–723. https://doi.org/10.1016/j.jcmg.2015.03.005 PMID: 26068288